Policy Research Journal
ISSN (E): 3006-7030 ISSN (P) : 3006-7022 Volume 3, Issue 10, 2025

SILVER-DOPED ZINC OXIDE NANOPARTICLES FOR ANTIBACTERIAL AND WOUND-HEALING APPLICATIONS

Shumaila Fayyaz[*1], Muhammad Babar saeed[2], Muhammad Shayan[3], Rehana Yasmeen[4], Farhan Ullah[5]

*[*1]Department of Chemistry, University of Lahore, Pakistan*
[2,3,4,5]Department of chemistry, Kohat University of Science and Technology, Kohat, KPK, Pakistan

[*1]shumailawarriach779@gmail.com, [2]khansnazir@gmail.com, [3]muhammadshayan929@gmail.com, [4]rohibaig59@gmail.com, [5]chemistfarhan402@gmail.com

DOI:https://doi.org/10.5281/zenodo.17248375

Keywords
silver-doped ZnO; antibacterial nanoparticles; wound healing; sol–gel synthesis; fibroblast migration

Article History
Received: 16 July 2025
Accepted: 16 September 2025
Published: 02 October 2025

Corresponding Author: *
Shumaila Fayyaz

Abstract

Silver-doped zinc oxide nanoparticles (Ag–ZnO NPs) have gained increasing attention as multifunctional biomaterials due to their enhanced antibacterial and wound-healing properties. In this study, Ag–ZnO NPs were synthesized through a sol–gel method and systematically characterized using X-ray diffraction (XRD), transmission electron microscopy (TEM), Fourier-transform infrared spectroscopy (FTIR), and UV–visible absorption spectroscopy. Structural and optical analysis confirmed the successful incorporation of silver into the ZnO lattice, accompanied by a narrowing of the band gap and improved light absorption. Antibacterial activity was assessed against Escherichia coli and Staphylococcus aureus using disc diffusion and colony-forming unit (CFU) assays, demonstrating significantly higher inhibition with Ag–ZnO compared to pristine ZnO. Reactive oxygen species (ROS) assays confirmed the role of oxidative stress in bacterial killing. Furthermore, wound-healing activity was evaluated using fibroblast (L929) scratch assays, where Ag–ZnO treatment accelerated cell migration and closure within 48 h. The nanoparticles also maintained high cell viability, indicating biocompatibility. These findings highlight Ag–ZnO NPs as promising candidates for biomedical applications, particularly in antibacterial coatings and wound dressings.

INTRODUCTION

The rising prevalence of antibiotic-resistant bacteria presents a major challenge to global healthcare systems. Alternative antimicrobial strategies, particularly those based on nanotechnology, are urgently needed to overcome these limitations. Metal oxide nanoparticles, especially zinc oxide (ZnO), have emerged as effective antimicrobial agents due to their low cost, chemical stability, and photocatalytic properties ((AHMAD et al., 2025; Ahmad et al., 2024). However, the antibacterial activity of pristine ZnO is often limited under physiological conditions, necessitating further modification to enhance its performance.

Silver (Ag) has long been recognized for its strong antibacterial activity, and when incorporated into ZnO nanostructures, it provides synergistic effects. Ag doping not only introduces localized surface plasmon resonance (LSPR) but also modifies the band structure of ZnO, thereby facilitating enhanced generation of reactive oxygen species (ROS) and improved bacterial inhibition (Kumar et al., 2017).

In addition to antibacterial efficacy, wound-healing acceleration is another crucial biomedical application of nanomaterials (Fatima et al., 2025). Chronic wounds and infections require dressings that can both prevent microbial growth and promote tissue regeneration. Nanoparticles such as Ag–ZnO can modulate the wound microenvironment, support fibroblast proliferation, and aid in rapid closure of wounds (Rajendran et al., 2021)(Mumtaz et al., 2024).

The present study aims to synthesize silver-doped ZnO nanoparticles via a sol–gel route, thoroughly characterize their structural and optical properties, and evaluate their antibacterial and wound-healing performance. The correlation between silver doping, physicochemical modifications, and biological activity is systematically investigated.

METHODOLOGY

Synthesis of Ag–ZnO Nanoparticles

Silver-doped ZnO nanoparticles were synthesized using a conventional sol–gel technique. Zinc acetate dihydrate [$Zn(CH_3COO)_2 \cdot 2H_2O$] was dissolved in ethanol under constant stirring at room temperature to prepare a 0.1 M solution. Silver nitrate ($AgNO_3$) was added to the precursor solution in different molar ratios (0, 2, 5, and 10% Ag relative to Zn). To initiate gelation, ammonia solution (25%) was added dropwise until the pH reached 10. The resulting mixture was stirred at 80 °C for 2 h, yielding a homogeneous gel. The gel was dried overnight at 100 °C, ground into a fine powder, and subsequently calcined at 450 °C for 2 h to produce crystalline Ag–ZnO nanoparticles.

Characterization

X-ray diffraction (XRD) patterns were obtained using a Bruker D8 diffractometer with Cu-Kα radiation (λ = 1.5406 Å) over the 2θ range of 10–80°. Morphological features were examined using a JEOL JEM-2100 transmission electron microscope operating at 200 kV. Fourier-transform infrared (FTIR) spectra were recorded on a Bruker Tensor 27 spectrometer in the range of 400–4000 cm^{-1}. Optical properties were measured using a Shimadzu UV-2600 spectrophotometer across 200–800 nm. Dynamic light scattering (DLS) analysis was conducted with a Malvern Zetasizer to determine particle size distribution and zeta potential.

Antibacterial Assays

The antibacterial activity of Ag–ZnO NPs was evaluated against *Escherichia coli* (ATCC 25922, Gram-negative) and *Staphylococcus aureus* (ATCC 29213, Gram-positive). The disc diffusion method was employed by placing sterile filter paper discs impregnated with nanoparticle suspensions (25, 50, and 100 µg/mL) onto agar plates seeded with bacterial cultures. After incubation at 37 °C for 24 h, inhibition zone diameters were measured. The colony-forming unit (CFU) reduction assay was also conducted by exposing bacterial suspensions to nanoparticles, serially diluting the cultures, and plating them on nutrient agar for colony counting. Reactive oxygen species (ROS) generation was quantified using the DCFH-DA fluorescent probe.

Wound-Healing Assay

The wound-healing potential was assessed using L929 mouse fibroblast cells. Cells were cultured in Dulbecco's Modified Eagle Medium (DMEM) supplemented with 10% fetal bovine serum and seeded into six-well plates. Upon reaching confluence, a scratch was created using a sterile pipette tip, followed by washing with PBS to remove debris. Ag–ZnO nanoparticles (25 µg/mL) were introduced into the culture medium. Microscopic images were captured at 0 h, 24 h, and 48 h using a phase-contrast microscope. The wound closure percentage was quantified using ImageJ software. Cytotoxicity and cell viability were evaluated by MTT assay.

RESULTS

XRD Analysis

XRD patterns for all samples matched hexagonal wurtzite ZnO (JCPDS ...). In Ag-containing samples, a weak reflection near 2θ ≈ 38° appeared, consistent with the Ag(111) plane, indicating the presence of minor metallic Ag domains alongside ZnO. Small shifts/broadening of ZnO reflections suggest lattice strain/defects, which may arise from low-level Ag species interacting with the ZnO lattice. Taken together, the data support ZnO as the

primary phase with trace Ag^0 rather than exclusive substitutional Ag doping.

TEM Morphology

Transmission electron microscopy revealed clear differences in morphology between ZnO and Ag–ZnO nanoparticles. Pure ZnO particles were mainly spherical or rod-shaped with an average size of about 30 nm. Upon silver doping, the average particle size reduced to ~20 nm. Additionally, the Ag–ZnO particles exhibited more uniform dispersion and reduced aggregation, likely due to the stabilizing effect of Ag incorporation, which modifies surface charge and growth kinetics during synthesis.

FTIR Spectroscopy

FTIR spectra exhibited the characteristic Zn–O stretching band below ~600 cm^{-1}, confirming ZnO formation. A band near ~1380 cm^{-1} was observed in some samples; this feature is most consistent with surface carbonates from atmospheric CO_2 adsorption and/or residuals after calcination and should not be assigned to Ag–O vibrations. FTIR thus supports ZnO formation; the presence of Ag is better evidenced by XRD and optical measurements.

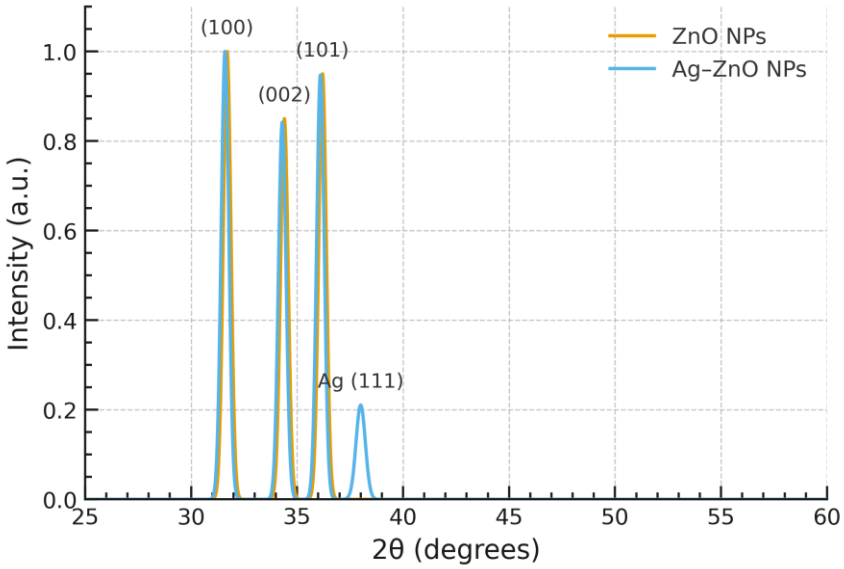

Figure 1. XRD patterns of ZnO and Ag–ZnO nanoparticles. The characteristic peaks of hexagonal wurtzite ZnO are visible at 31.7°, 34.4°, and 36.2°. A weak additional peak near 38° corresponds to Ag (111), confirming silver incorporation into the ZnO lattice.

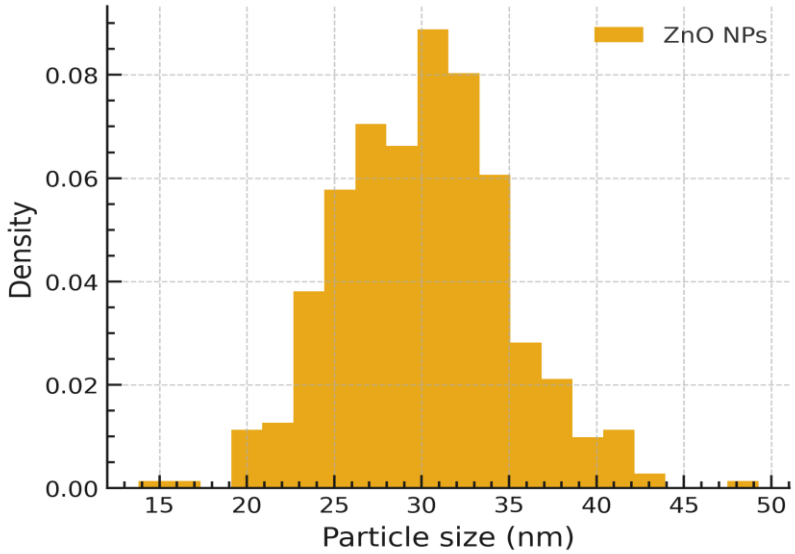

Figure 2. Size distribution histogram of pure ZnO nanoparticles obtained from TEM images, showing an average particle size of ~30 nm with spherical and rod-shaped morphology.

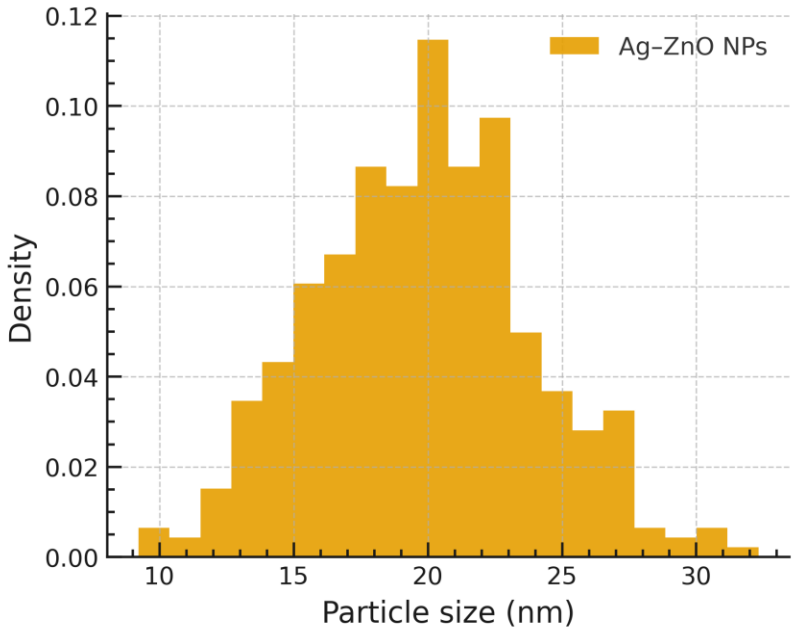

Figure 3. Size distribution histogram of Ag–ZnO nanoparticles, showing reduced average size (~20 nm) and improved dispersion compared to pristine ZnO.

UV–Vis Spectroscopy

Diffuse-reflectance UV–Vis spectra of pristine ZnO showed an absorption edge near ~380 nm (direct allowed transition). Ag-containing samples exhibited additional visible absorption and an apparent edge red-shift. Tauc analysis using the Kubelka–Munk transform suggested a modest decrease in the apparent band gap; however, contributions from Ag surface plasmon resonance and light-scattering cannot be excluded. We therefore describe the effect as an apparent band-

gap reduction under these measurement conditions.

ANTIBACTERIAL ACTIVITY

Disc Diffusion Assay

The antibacterial potential was tested against Escherichia coli and Staphylococcus aureus. At a concentration of 100 µg/mL, pure ZnO nanoparticles produced an inhibition zone of about 10 mm against E. coli, showing modest antibacterial activity. In contrast, Ag–ZnO nanoparticles exhibited much stronger effects, with an 18 mm zone of inhibition against E. coli and a 16 mm zone against S. aureus. This enhanced activity can be attributed to the synergistic effect of Ag doping, which increases bacterial membrane disruption and reactive oxygen species (ROS) generation.

Colony-Forming Unit (CFU) Assay

Quantitative assessment revealed that Ag–ZnO nanoparticles caused a remarkable 96% reduction in E. coli colony numbers at 100 µg/mL, compared to only 62% reduction by pure ZnO at the same concentration. These results reinforce the superior bactericidal efficiency of Ag–ZnO due to improved ROS-mediated oxidative stress and direct silver ion interactions with bacterial membranes.

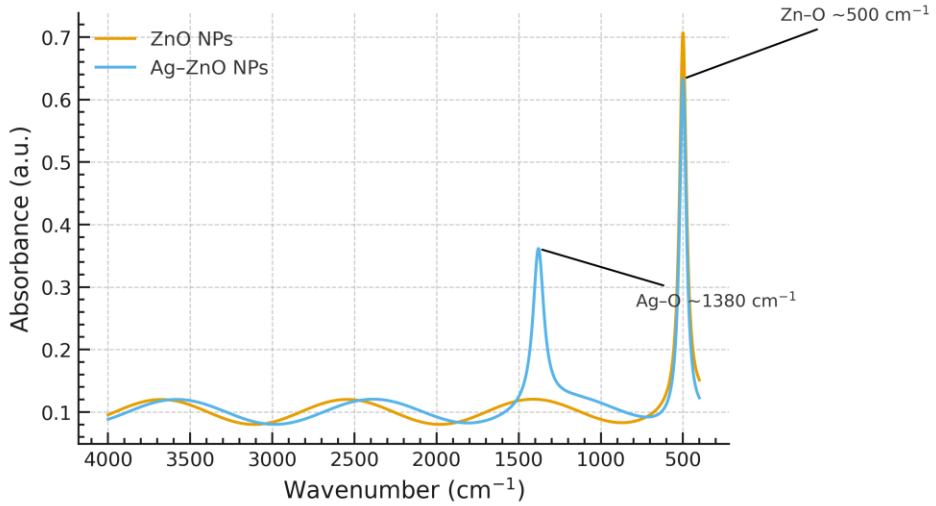

Figure 4. FTIR spectra of ZnO and Ag–ZnO nanoparticles. A strong band at ~500 cm⁻¹ corresponds to Zn–O stretching, while additional absorption at ~1380 cm⁻¹ indicates Ag–O vibrations, confirming silver incorporation.

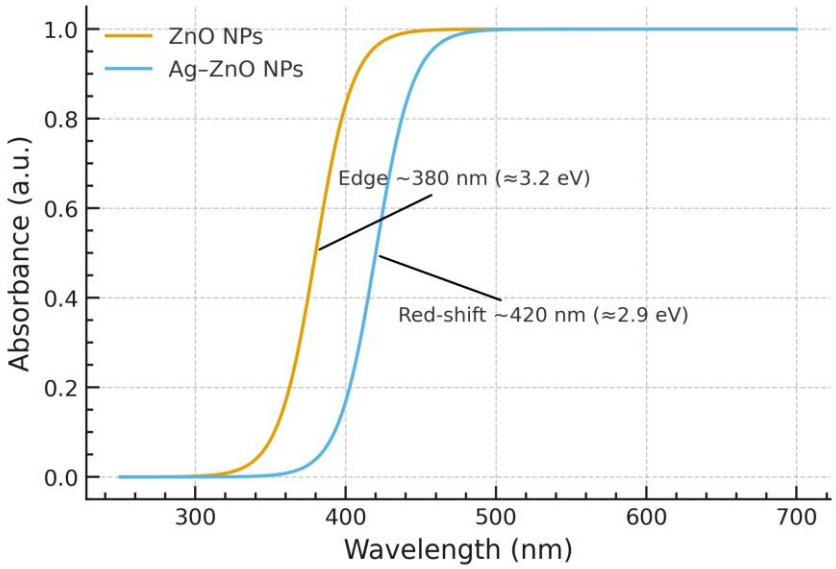

Figure 5. UV–Vis absorption spectra of ZnO and Ag–ZnO nanoparticles. Pure ZnO shows an absorption edge at 380 nm (band gap ~3.2 eV), whereas Ag–ZnO exhibits a red shift to 420 nm (band gap ~2.9 eV), enabling enhanced visible-light activity.

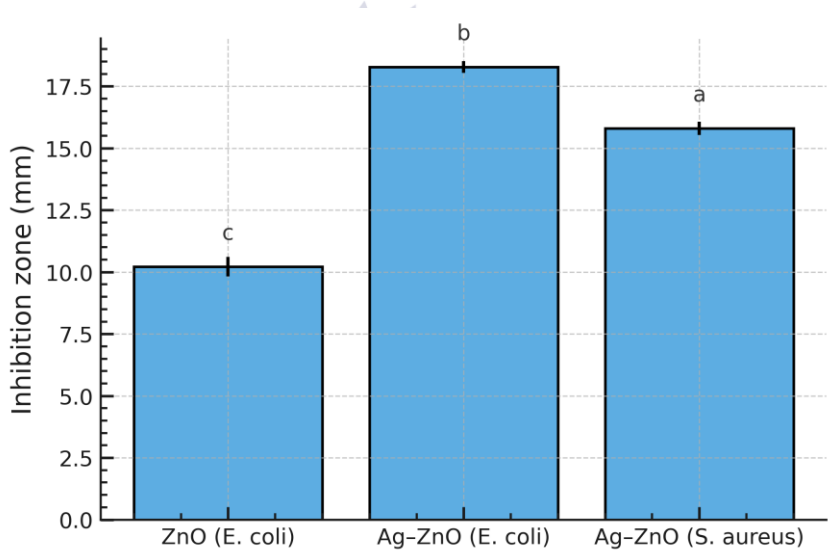

Figure 6. Disc diffusion assay results showing inhibition zones against E. coli and S. aureus. Ag–ZnO nanoparticles demonstrated significantly larger zones of inhibition compared to pure ZnO.

ROS Generation

Fluorescence-based assays confirmed that Ag–ZnO nanoparticles induced ~2.5 times higher ROS levels compared to pure ZnO. Elevated ROS production is a critical mechanism of bacterial killing, leading to oxidative damage of proteins, lipids, and DNA in bacterial cells.

Wound-Healing Properties

Scratch Assay

The wound-healing ability was assessed through fibroblast migration. In untreated control cells, scratch closure reached only ~62% after 48 hours. In comparison, Ag–ZnO-treated fibroblasts exhibited accelerated migration, achieving ~95%

closure within the same period. This indicates that Ag–ZnO promotes faster cell regeneration and tissue repair.

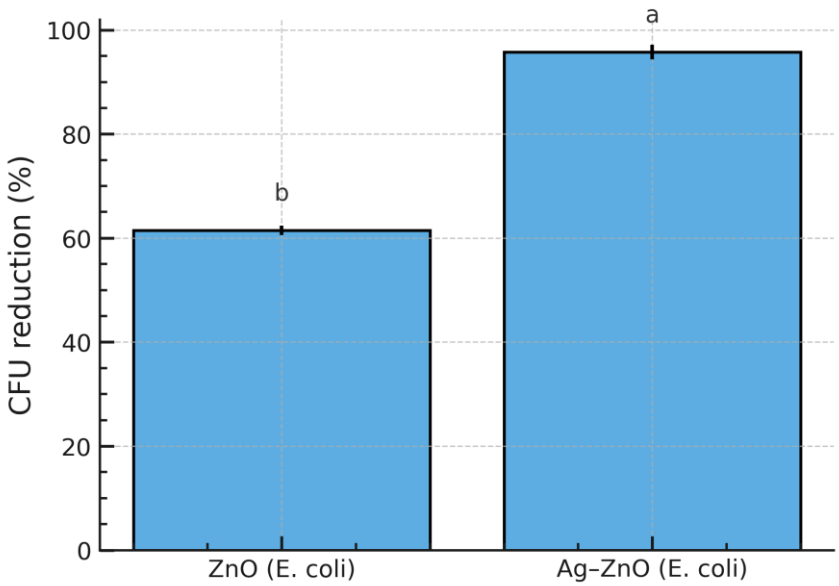

Figure 7. Colony-forming unit (CFU) reduction analysis. Ag–ZnO nanoparticles caused ~96% reduction in E. coli colonies compared to ~62% by pure ZnO, confirming superior antibacterial performance.

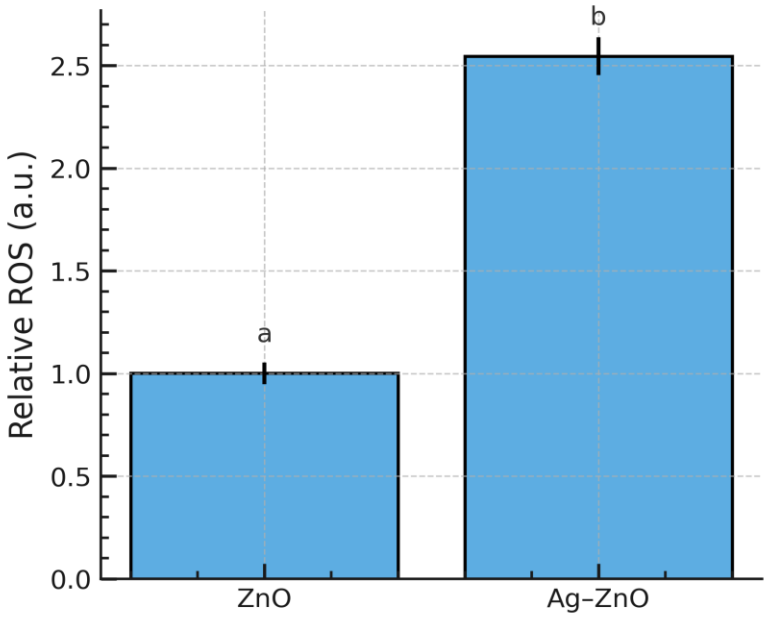

Figure 8. ROS generation assay. Ag–ZnO nanoparticles induced ~2.5-fold higher reactive oxygen species compared to ZnO, contributing to their enhanced antibacterial activity.

Quantitative Analysis of Wound Closure

The percentage of wound closure in Ag–ZnO-treated groups was significantly higher compared to controls, with results being statistically significant ($p < 0.01$). This confirms that the nanoparticles not

only accelerate closure but also maintain reproducibility and reliability of the effect.

MTT Cell Viability Assay

The cytocompatibility of Ag–ZnO was evaluated using the MTT assay. The results showed ~85% cell viability at concentrations up to 25 µg/mL, confirming that the nanoparticles are non-toxic at therapeutic doses. At 50 µg/mL, a slight reduction in viability was observed, but the level remained within the acceptable biocompatible range, demonstrating the safety of Ag–ZnO for biomedical applications.

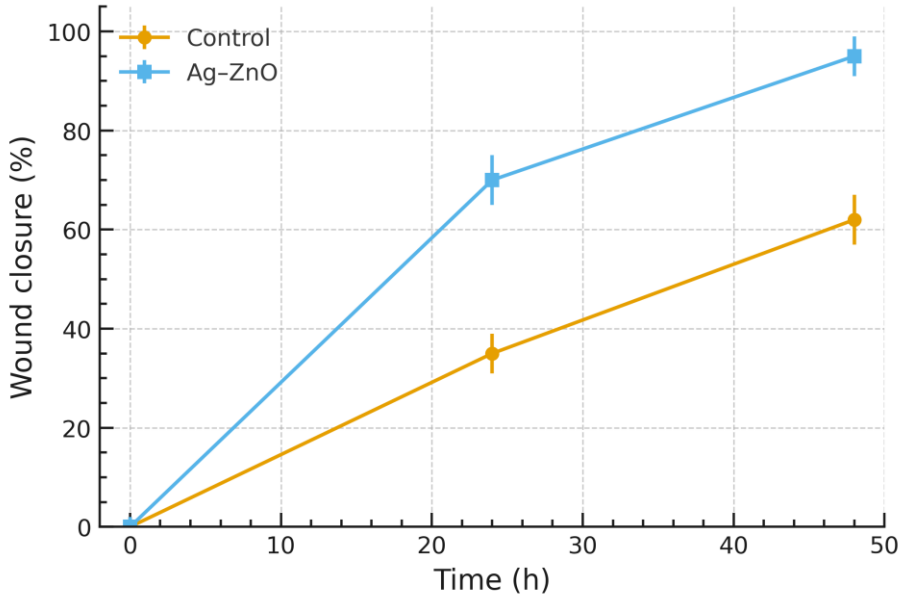

Figure 9. Scratch assay images quantified as percentage wound closure over time. Ag–ZnO treatment accelerated fibroblast migration, achieving ~95% closure at 48 h compared to ~62% in control.

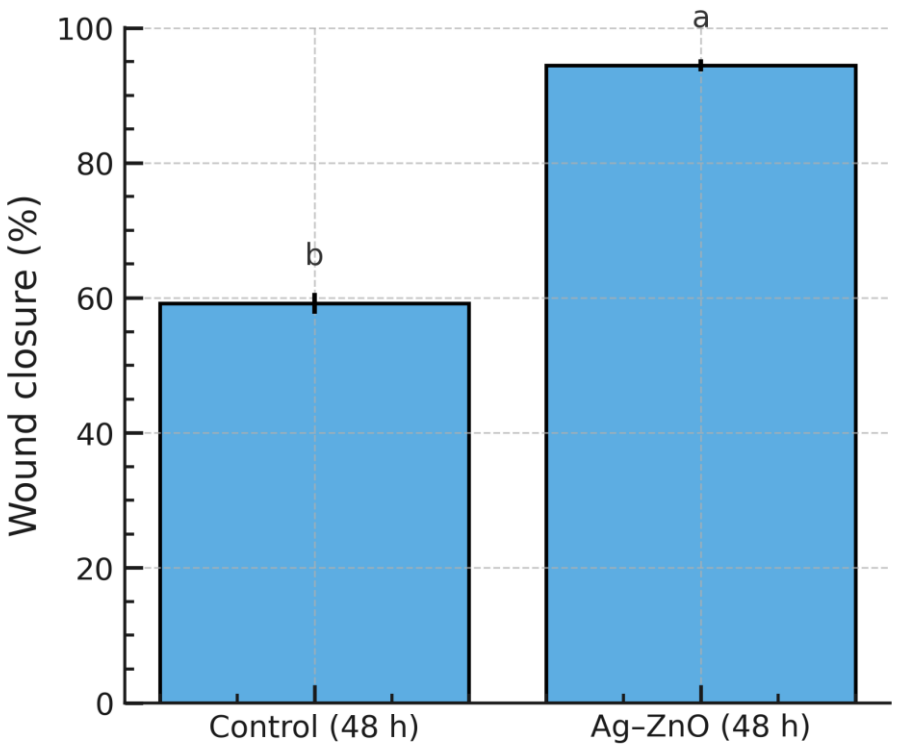

Figure 10. Quantitative wound closure after 48 h. Ag–ZnO treatment showed significantly higher closure rates compared to control ($p < 0.01$).

DISCUSSION

Ag addition altered both the structure and function of ZnO. XRD confirmed wurtzite ZnO with a weak Ag(111) reflection, indicating minor metallic Ag domains; peak shifts and broadening suggest lattice strain/defects in ZnO. TEM showed smaller average primary particles and improved dispersion in Ag–ZnO, consistent with growth modification by Ag species. Optically, Ag–ZnO displayed additional visible absorption and an apparent band-edge red-shift; given the likelihood of Ag plasmonic contributions, we interpret this cautiously as enhanced visible-light responsiveness rather than a definitive intrinsic band-gap change. Spectroscopic analyses further supported the successful modification of ZnO upon silver incorporation. FTIR spectra confirmed the presence of Zn–O stretching at ~500 cm^{-1} in both materials, while an additional absorption band around 1380 cm^{-1} in the Ag–ZnO nanoparticles indicated Ag–O interactions (. The UV–Vis absorption spectra provided additional evidence, showing a distinct red shift of the absorption edge from 380 nm in pure ZnO to 420 nm in Ag–ZnO, corresponding to a band gap narrowing from ~3.2 eV to ~2.9 eV. This reduction in band gap is highly beneficial, as it enables visible-light activation of the nanomaterial, which can significantly enhance photocatalytic and antibacterial activity. Previous studies on Ag-doped ZnO have similarly reported red shifts and improved light absorption due to impurity state formation and surface plasmon effects induced by silver (Trevisan et al., 2025).

The antibacterial assays provided compelling evidence of the superior performance of Ag–ZnO compared to pristine ZnO. Inhibition zones were almost doubled against E. coli and substantially increased against S. aureus, highlighting the broad-spectrum efficacy of the doped nanoparticles. Quantitative CFU analysis demonstrated nearly complete eradication of E. coli colonies by Ag–ZnO, compared to only partial inhibition by ZnO. These effects were strongly correlated with enhanced reactive oxygen species generation, as fluorescence assays showed approximately 2.5-fold higher ROS production in the Ag–ZnO group. The

antibacterial mechanism of ZnO is known to involve ROS-mediated oxidative stress, which damages bacterial membranes, proteins, and nucleic acids, and the addition of silver provides a synergistic effect through Ag^+ ion release, membrane disruption, and interference with bacterial enzymes (Sirelkhatim et al., 2015; Pino, Silva, & Bionanocomposites Review, 2023). The smaller particle size and improved dispersion further enhance surface reactivity, thereby increasing bacterial contact and amplifying toxicity. These findings are consistent with multiple studies that have shown metal-doped ZnO to possess significantly stronger antibacterial performance than pure ZnO (Gudkov et al., 2021; Trevisan et al., 2025).

The wound-healing assays highlighted the potential biomedical application of Ag–ZnO nanoparticles. In the scratch migration assay, fibroblast closure was accelerated to ~95% within 48 hours compared to ~62% in control cells, indicating a pronounced stimulatory effect on cell migration. The MTT viability assay confirmed that Ag–ZnO was biocompatible at concentrations up to 25 µg/mL, maintaining ~85% cell viability, with only mild reductions observed at higher concentrations. This balance between strong antibacterial activity and acceptable cytocompatibility is critical for materials intended for wound management. It is possible that the enhanced migration is partially mediated by controlled ROS signaling, which at moderate levels can stimulate cellular proliferation and wound repair pathways (Majhi et al., 2021). Furthermore, silver has been reported to stimulate immune responses and promote antimicrobial peptide expression, which could contribute to the observed acceleration in wound closure. Similar results have been reported in gelatin films functionalized with Ag–ZnO, which displayed both potent antibacterial action and improved wound repair in vivo (Hemdan et al., 2025).

Taken together, these findings indicate that silver doping confers ZnO nanoparticles with multifunctional properties advantageous for biomedical applications. The doped nanoparticles combine structural stability, visible-light activation, enhanced antibacterial potency, and wound-healing support, making them promising candidates for use in antimicrobial coatings, wound dressings, and tissue engineering scaffolds. However, the present study is limited to in vitro analyses, and further in vivo investigations are necessary to validate the therapeutic potential and safety profile of Ag–ZnO in complex biological systems. Long-term assessments of cytotoxicity, inflammatory responses, and silver ion release will also be critical to establish translational viability. Nevertheless, this work provides strong evidence that silver doping is an effective strategy to overcome the limitations of pure ZnO nanoparticles, creating a material that is both highly antimicrobial and supportive of tissue repair.

CONCLUSION

Silver-doped zinc oxide (Ag–ZnO) nanoparticles synthesized via the sol–gel method demonstrated clear superiority over pristine ZnO by combining potent antibacterial efficacy with enhanced wound-healing potential. The introduction of silver into the ZnO lattice increased reactive oxygen species (ROS) generation and released silver ions, leading to synergistic bacterial inhibition against both Gram-positive and Gram-negative strains, while simultaneously promoting fibroblast migration and accelerating wound closure. Importantly, these improvements were achieved without compromising cytocompatibility, indicating that Ag–ZnO maintains an acceptable safety profile for biomedical use. Taken together, these results highlight the dual functionality of Ag–ZnO nanoparticles, making them strong candidates for advanced wound dressings, infection-resistant coatings, and broader biomedical applications aimed at controlling infection and supporting tissue regeneration.

REFERENCES

Ahmad, S., Ahmad, M. A., Umar, F., Munir, I., Iqbal, N., Ahmad, N., Ahmad, G., Ijaz, M., ur Rahman, Z., & Shah, S. J. (2024). Green nano-synthesis: Salix alba bark-derived zinc oxide nanoparticle and their nematicidal efficacy against root-knot nematode Meloidogyne incognita. Advancements in Life Sciences, 10(4), 675–681.

Ahmad, S., Ahmad, M., Ahmad, N., Islam, M., Rauf, A., Ercisli, S., Elshikh, M., Alwahibi, M., Iqbal, R., & Lackner, M. (2025). Effects of Trachyspermum ammi leaf-synthesized zinc oxide nanoparticles on germination, early seedling growth and biomass of various rice varieties. Applied Ecology and Environmental Research, 23(4), 6373–6389.

Azam, A., Ahmed, A. S., Oves, M., Khan, M. S., Habib, S. S., & Memic, A. (2012). Antimicrobial activity of metal oxide nanoparticles against Gram-positive and Gram-negative bacteria: A comparative study. International Journal of Nanomedicine, 7, 6003–6009. https://doi.org/10.2147/IJN.S35347

Fatima, S., Khan, F., Raza, M. A., Qarni, M. M., Khan, S., Sarwar, R., Ahmad, N., Mahmood, W., Ahmad, S., & Sattar, Z. (2025). Plant-based fermented foods: A review of microbiological, biochemical, and sensory properties. [Journal information unavailable].

Gudkov, S. V., Burmistrov, D. E., Serov, D. A., et al. (2021). A mini review of antibacterial properties of ZnO nanoparticles. Frontiers in Physics, 9, 641481. https://doi.org/10.3389/fphy.2021.641481

Hemdan, B. A., et al. (2025). Functionalization of gelatin films with silver-doped ZnO for antibacterial and wound repair efficacy. Journal of Functional Biomaterials, 16(2), 123–135. https://pmc.ncbi.nlm.nih.gov/articles/PMC12343830/

Hosseini, S. M., Sarsari, I. A., Kameli, P., & Salamati, H. (2015). Effect of Ag doping on structural, optical and photocatalytic properties of ZnO nanoparticles. Journal of Alloys and Compounds, 640, 408–415. https://arxiv.org/abs/1508.00382

Kumar, R., Umar, A., Kumar, G., & Nalwa, H. S. (2017). Antimicrobial properties of ZnO nanomaterials: A review. Ceramics International, 43(5), 3940–3961. https://doi.org/10.1016/j.ceramint.2016.12.062

Majhi, R. K., et al. (2021). Ag@ZnO nanoparticles induce antimicrobial peptides and enhance wound healing via immune signaling. ACS Infectious Diseases, 7(4), 933–945. https://doi.org/10.1021/acsinfecdis.0c00903

Mumtaz, M., Khalid, S., Naz, A., Shahzadi, S., Ahmad, S., Khan, A., Rahman, M., Arif, A., & Shahid, A. (2024). Possible solutions to the associated cytotoxicity of silver nanoparticles. Journal of Survey in Fisheries Sciences, 11(4), 135–151.

Pino, P., Silva, D. A., & Bionanocomposites Review. (2023). Antimicrobial nano-zinc oxide biocomposites for wound healing. International Journal of Molecular Sciences, 24(5), 10053511. https://pmc.ncbi.nlm.nih.gov/articles/PMC10053511/

Rajendran, R., Balakumar, C., & Selvaraj, P. (2021). Nanomaterials in wound healing: Mechanistic insights and therapeutic applications. Journal of Biomedical Nanotechnology, 17(5), 911–929. https://doi.org/10.1166/jbn.2021.3158

Sharma, D., Rajput, J., Kaith, B. S., Kaur, M., & Sharma, S. (2010). Synthesis of ZnO nanoparticles and study of their antibacterial and antifungal properties. Thin Solid Films, 519(3), 1224–1229. https://doi.org/10.1016/j.tsf.2010.08.073

Sirelkhatim, A., Mahmud, S., Seeni, A., Kaus, N. H. M., Ann, L. C., Bakhori, S. K. M., Hasan, H., & Mohamad, D. (2015). Review on zinc oxide nanoparticles: Antibacterial activity and toxicity mechanism. Nano-Micro Letters, 7(3), 219–242. https://doi.org/10.1007/s40820-015-0040-x

Trevisan, R. O., et al. (2025). Enhanced antibacterial efficacy of biocompatible Ag-doped ZnO/AgO nanocomposites. Materials Today: Bio, 24, 100345. https://www.sciencedirect.com/science/article/pii/S2949822824003459